Available online at www.sciencedirect.com

ScienceDirect

journal homepage: www.intl.elsevierhealth.com/journals/dema

# Three-dimensional assessment of proximal contact enamel using optical coherence tomography

*Thwe Zin Ei*[a], *Yasushi Shimada*[a,b,*], *Ahmed Abdou*[a,c], *Alireza Sadr*[a,d], *Masahiro Yoshiyama*[b], *Yasunori Sumi*[e], *Junji Tagami*[a]

[a] *Department of Cariology and Operative Dentistry, Division of Oral Health Science, Graduate School of Medical and Dental Sciences, Tokyo Medical and Dental University, Tokyo, Japan*

[b] *Department of Operative Dentistry, Graduate School of Medicine, Dentistry and Pharmaceutical Sciences, Okayama University, Okayama, Japan*

[c] *Biomaterials Department, Faculty of Oral and Dental Medicine, Modern University for Technology and Information, Cairo, Egypt*

[d] *Biomimetics Biomaterials Biophotonics Biomechanics & Technology Laboratory, Department of Restorative Dentistry, University of Washington, Seattle, WA, USA*

[e] *Center of Advanced Medicine for Dental and Oral Diseases, Department for Advanced Dental Research, National Center for Geriatrics and Gerontology, Aichi, Japan*

ARTICLE INFO

*Article history:*
Received 18 August 2018
Received in revised form
27 November 2018
Accepted 11 January 2019

*Keywords:*
Optical coherence tomography
3D imaging
Proximal contact
Enamel
Microcrack
Demineralization
International Caries Detection and Assessment System (ICDAS)

ABSTRACT

*Objective.* The purpose of this study was to detect and investigate the association of enamel microcracks with demineralization at proximal contact areas of premolars, using 3D swept-source optical coherence tomography (SS-OCT).

*Methods.* Extracted maxillary and mandibular premolars (n = 50 each), without any visible tooth cracks, were examined for demineralization of interproximal contact areas, using the International Caries Detection and Assessment System (ICDAS). SS-OCT was used to evaluate demineralization and detect microcracks. Demineralization progression was divided into 4 types by depth: 0 for sound enamel and Type I, II, and III for enamel demineralization penetrating into the outer third, the middle third, and the inner third of the enamel thickness, respectively. Enamel microcracks were classified according to the predominant crack pattern: Type O, no cracks; Type A, subsurface microdefects; Type B, enamel microcrack running along the direction of the enamel prism; Type C, enamel microcrack running transverse to the enamel prism direction; and Type D, a combination of patterns A, B, and C. SS-OCT findings were confirmed by confocal laser scanning microscopy observation.

*Results.* Microcracks confined within the superficial enamel in proximal contact areas were seen as bright lines on SS-OCT. There were significant positive correlations among ICDAS codes, demineralization levels, and microcrack distribution ($p \leq 0.001$). The mesial side of maxillary premolars showed significantly more demineralization (n = 36) and microcracks (n = 27) than that of the mandibular premolars (n = 20 and n = 14, respectively; $p < 0.001$).

* *Corresponding author at*: Department of Operative Dentistry, Okayama University, 2-5-1 Shikata-cho, Kita-ku, Okayama 700-8525, Japan.
E-mail address: shimada.ope@okayama-u.ac.jp (Y. Shimada).

https://doi.org/10.1016/j.dental.2019.01.008

*Significance.* The presence of microcracks within the superficial enamel in proximal contact areas could be determined using SS-OCT, and correlated with the level of demineralization. 3D SS-OCT is a valuable diagnostic tool for comprehensive assessment of microstructural changes related to enamel demineralization and crack development.



## 1. Introduction

Dental caries is a biofilm-mediated, sugar-driven, multifactorial, dynamic disease that results in the phasic demineralization and remineralization of dental hard tissues [1]. Due to widespread fluoride accessibility over the past few decades, the incidence of caries has markedly declined and the pattern of lesions changed [2]. Although there has been a distinct reduction in development of enamel caries on smooth surfaces, carious lesions remain highly localized on the occlusal and proximal surfaces of the posterior teeth [3,4]. It has also been reported that a greater proportion of caries lesions are detected on the proximal surfaces of the teeth when radiographically examined than when only examined clinically, particularly in a young adult population [5,6].

Proximal surfaces, which are usually in contact with adjacent teeth under physiological circumstances, are highly exposed to the carious process [7]. During mastication, the teeth are tipped mesially; a gliding movement between contacting surfaces results in wear and in the development of a proximal contact area [8,9]. Moreover, excessive proximal tooth contact provides increased tightness and affects the tensile stress at the proximal contact areas [10,11]. It has been reported that compressive, shear, and tensile stresses produced during mastication cause enamel wear on the contact surface [12]. Depending on the contact stress, wear can inhibit or enhance the formation of cracks [13]. However, to date, no study has focused on detection of enamel cracks in the interproximal contact area, except for the developmental lamella [14].

Unlike the occlusal and free smooth surfaces, the arch alignment and the presence of neighboring teeth prevent visual exanimation of the proximal surfaces. Difficulty in accessing the proximal area for diagnostic evaluation may result in underestimation of the caries prevalence, especially in young adults [6]. Moreover, for early detection of approximal caries, the clinician usually relies on bitewing radiographs and visual inspection [15,16]. Although these are well-accepted as useful diagnostic methods with high specificity, their low sensitivity may lead to underestimation of the lesion extent [17]. In recent years, the International Caries Detection and Assessment System (ICDAS) has been introduced as a new protocol for dental caries assessment [18]. This system helps to standardize visual diagnosis, provides early detection of caries with respect to existing color changes or surface moisture, and has been validated against histological examination of occlusal caries. Moreover, the ICDAS have been reported to be an accurate method for detecting and estimating the depth of proximal lesions in open inspection [19]. However, in a clinical situation, its reliability in the smooth approximal surface still requires validation against other supplementary diagnostic tools.

Optical coherence tomography (OCT) has been developed as a non-invasive, cross-sectional imaging system that can visualize internal structures non-destructively [20]. OCT is based on the concept of low-coherence interferometry, where the backscattered signal intensity projected onto the sample reveals depth-resolved information about the scattering and reflection of light in the sample [21]. Swept-source OCT (SS-OCT) is the latest enhancement of that imaging technology, in which the laser source sweeps the target with near-infrared wavelengths, within millisecond-scan delays, at kilohertz rates, to achieve real-time imaging. With enhanced image resolution and scanning speed for 2D and 3D images, it has been used in the detection of carious lesion, cracks, and dental restoration defects [13,22,23]. Moreover, SS-OCT has been reported to demonstrate high sensitivity and specificity for early detection of smooth surface caries [24] and proximal caries [25].

As caries lesions develop and spread in 3 dimensions, early detection of caries by using SS-OCT with 3D imaging will be clinically useful. Moreover, a better understanding of the nature and development of lesions during the early stage is important for gaining insight into the etiology of the disease, as well as for implementing preventive and interceptive treatment strategies. Therefore, this study aimed to detect the initial demineralization and crack patterns in the proximal contact area of extracted human premolars using 3D SS-OCT. The caries susceptibility and lesion patterns were also evaluated by determining whether there were correlations among the visual assessment using ICDAS criteria, level of demineralization and crack pattern.

## 2. Materials and methods

The protocol was approved by the ethical review board and human research ethics committee of Tokyo Medical and Dental University. Fifty human premolars from each arch (maxilla and mandible) were examined in this study. The teeth were extracted for orthodontic purposes from individuals within the age range of 18–35 years. Inclusion criteria included sound teeth without any visible tooth cracks or craze lines, with no visible decalcification, or visible white spot-like changes on the smooth enamel of the proximal surfaces. The teeth were cleaned with prophylactic paste (Pressage, Shofu Inc., Kyoto, Japan) using a low-speed handpiece and were stored in distilled water containing thymol crystal. All the specimens were kept in a moist condition throughout the study, to prevent desiccation.

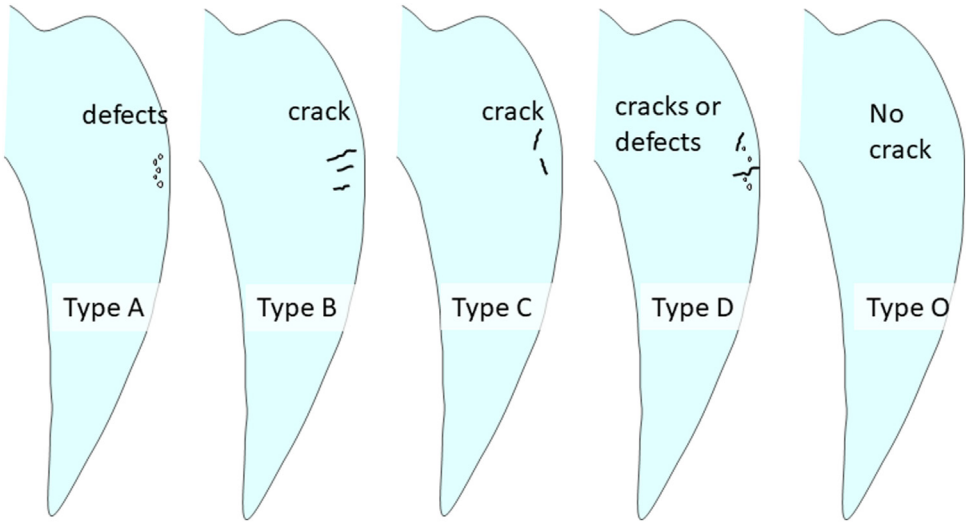


**Fig. 1 – Schematic illustrations of the different types of enamel microcracks.**
**Type A: microdefects at the subsurface enamel. Type B: microcrack running along the direction of the enamel prism. Type C: microcracks running transverse to the enamel prism direction. Type D: enamel cracks combining any of the patterns above. Type O: no micro-defects and micocracks. DEM: demineralization.**

### 2.1. *International Caries Detection and Assessment System (ICDAS)*

The interproximal contact areas of all teeth were visually inspected by a clinician, using the ICDAS criteria [18]:

1 *Sound enamel, with no change in translucency after prolonged (>5 s) air drying.*
2 *First visual changes visible in enamel; opacity or discoloration not visible on the wet surface, but distinctively visible after air drying, or seen on a wet surface.*
3 *Distinct visual changes in enamel; opacity or discoloration distinctly visible on a wet surface.*

### 2.2. *3D SS-OCT imaging*

The SS-OCT system (prototype, Yoshida Dental MFG, Tokyo, Japan) used in this study constructs a 3D image with a central wavelength of 1310 nm, a scan range of 140 nm, optical resolution in air of 11 μm in depth and 40 μm in width and length [13]. First, all surfaces of each extracted tooth were comprehensively observed using 3D SS-OCT imaging to confirm the absence of any mechanical damage to the tooth surface during the extraction process. Then, a handheld scanning probe was set to a fixed distance over the tooth, with the scanning beam oriented 90° to the interproximal surface. The tooth was examined at the interproximal contact area of both mesial and distal surfaces and observed for the presence of demineralized lesions or microcracks. 3D images, as well as 2D images along the x-, y-, and z-axes, were taken of the entire interproximal surface.

Demineralization progression was divided into 4 levels, according to the OCT light scattering lesion front and the enamel thickness:

*DEM Type 0: Sound tooth surface, in which the OCT signal at the interproximal contact area was of the same level as that of the surrounding normal enamel.*

*DEM Type I: Demineralization progression in the outer third of the enamel layer.*

*DEM Type II: Demineralization progression in the middle third of the enamel layer*

*DEM Type III: Demineralization progression in the inner third of the enamel layer, or near the dentinoenamel junction (DEJ).*

Enamel microcracks localized at the interproximal contact area were divided into 4 patterns (Fig. 1):

*Type A: Microdefects at the subsurface enamel.*

*Type B: Microcracks running in the direction of the enamel prism.*

*Type C: Microcracks running transverse to the enamel prism direction.*

*Type D: Enamel microcracks combining any of the above patterns.*

*Type O: No microdefects or microcracks observed.*

### 2.3. *Confocal laser scanning microscopy observations*

In order to validate the result of 3D and 2D OCT images, teeth were sectioned and examined by confocal laser scanning microscopy (CLSM) (VK-X150 series, Keyence, Osaka, Japan). The desired cross-sectional slides of the 3D OCT image were marked on the teeth and then the area of interest was sectioned using a low-speed diamond saw (Isomet, Buehler, Lake Bluff, IL, USA) under running water. The sectioned teeth were further trimmed using 2000-grit silicon carbide paper and polished down to 1 μm. The polished specimens were ultra-sonicated with distilled water for 3 min to remove the polishing debris and were examined by CLSM at 5× magnification.

### 2.4. *Statistical analysis*

The correlations of the ICDAS code with the demineralization level and crack pattern were assessed using Spearman's

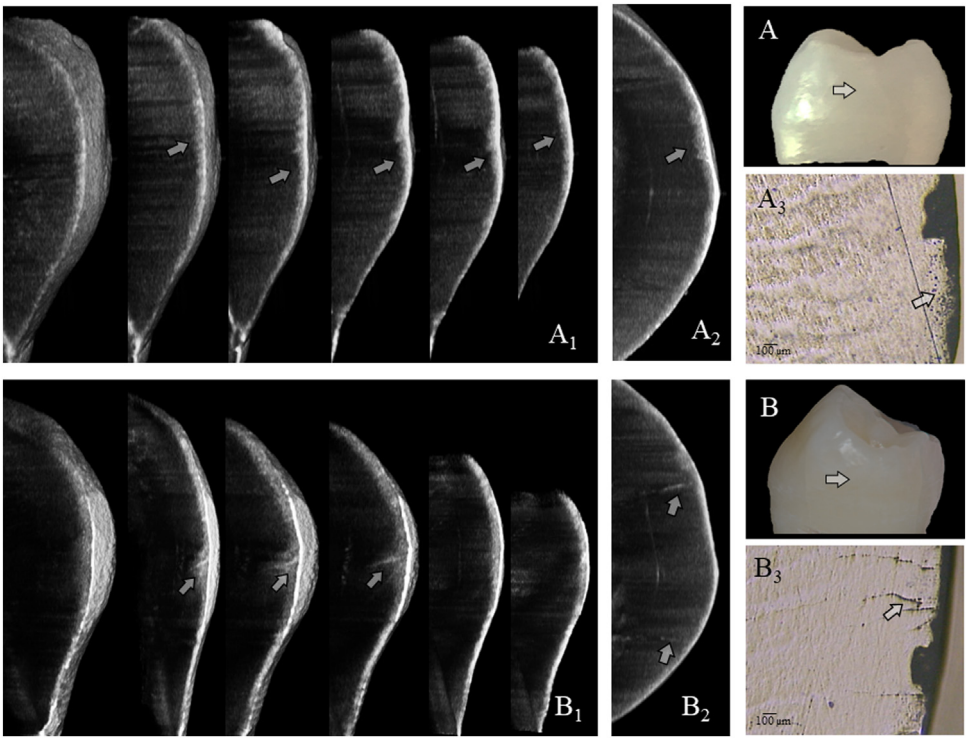


**Fig. 2 – Photographs, optical coherence tomography (OCT) images and confocal laser scanning microscopy (CLSM) images representative of demineralization and microcrack patterns. Photograph of sound maxillary premolar with ICDAS code 0 (A, the arrow indicates the region and direction of OCT scanning); SS-OCT images showing initial changes in the superficial enamel with Type A crack ($A_1$, Mesio-distal multiplanar view), ($A_2$, occluso-gingival view); CLSM images ($A_3$, the arrow indicates the Type A crack pattern); photograph of mandibular premolar, ICDAS code 1 (B, the arrow indicates the region and direction of OCT scanning); SS-OCT images showing Type I demineralization with Type B crack ($B_1$, Mesio-distal multiplanar view), ($B_2$, occluso-gingival view), CLSM images ($B_3$, the arrow indicates the Type B crack pattern).**

correlation analysis. The Kruskal–Wallis test was used for comparisons between maxillary and mandibular teeth on both sides, for each score, followed by the Dunn–Bonferroni post-hoc test for pairwise comparisons. Statistical analyses were performed using SPSS® IBM® (IBM SPSS Statistics for Windows, Version 23.0. Armonk, NY: IBM Corp.) Significance was set at $\alpha = 0.05$.

## 3. Result

After SS-OCT observation, one maxillary and one mandibular tooth were excluded due to enamel fracture during the tooth extraction process. Demineralized lesions presented as high reflectivity of enamel around the interproximal contact areas (Figs. 2 and 3). The typical lesion pattern appeared as a cone shape, with the base reaching from the enamel surface to DEJ, but some lesions presented only a superficial layer-type lesion pattern. Enamel microcracks were found together with demineralized interproximal contact areas in some teeth. These microcracks appeared as a bright line in SS-OCT, with 1 of 4 predominant patterns (Figs. 2 and 3).

Spearman's correlation analysis revealed significant positive correlations among ICDAS codes, demineralization levels, and microcrack distribution ($p \leq 0.001$). The distribution percentages of each parameter are described in Table 1. In Fig. 4, DEM and ICDAS scores showed a good agreement: DEM Type 0 corresponded to ICDAS code 0 (n = 91, 98.8%). Moreover, ICDAS code 1 clustered with DEM Type I (n = 33, 78.6%), while ICDAS code 2 was distributed between DEM Types II and III (n = 53, 85.5%). On the other hand, DEM Types 0 and I were either associated with Type O (no cracks; n = 81, 74.3%) or with type A cracks (n = 48, 82.7%). Type C and D cracks were only observed with DEM Types II (n = 4,100%) and III (n = 14, 100%); however, DEM Type II was associated with all types of cracks [O:,2 (36.4%), A: 7 (21.2%), B: 6 (18.2%), C: 4 (12.1%), and D: 4 (12.1%)]. In DEM Type III, Type O (n = 16, 55.2%) and type D (n = 10, 34.5%) cracks had the highest frequency.

The enamel microcrack distribution correlated with the demineralization lesion (Figs. 2 and 3). SS-OCT observations were validated by CLSM images. Pairwise comparison between mesial (U-M) and distal (U-D) contact areas of the maxillary, and mesial (L-M) and distal (L-D) contact areas of the mandibular teeth in each scoring parameter is described in Table 2. U-M showed significantly higher ICDAS Scores (code 2: 59.2%) among all the examined teeth ($p < 0.001$). The demineralization distribution was also significantly higher than that of L-M and L-D ($p < 0.001$). Although there was no significant difference in microcrack distribution between the mesial and distal side of the maxillary and mandibular teeth, U-M showed a significantly higher percentage of microcracks than L-M ($p = 0.032$).

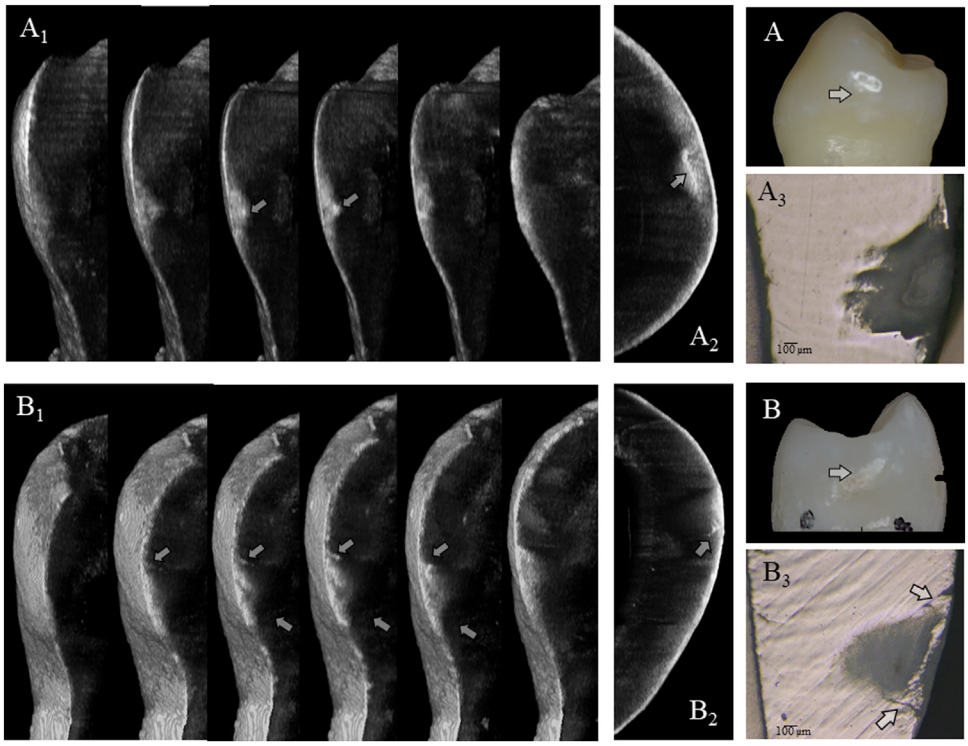


**Fig. 3 – Photographs, optical coherence tomography (OCT) images and confocal laser scanning microscopy (CLSM) images representative of demineralization and microcrack patterns. Photograph of mandibular premolar with ICDAS code 1 (A, the arrow indicates the region and direction of OCT scanning); SS-OCT images showing Type II demineralization with Type C crack ($A_1$, Mesio-distal multiplanar view), ($A_2$, occluso-gingival view); CLSM images ($A_3$, the arrow indicate the Type C crack pattern). Photograph of maxillary premolar, ICDAS code 2 (B, the arrow indicates the region and direction of OCT scanning), SS-OCT images showing Type III demineralization with Type D crack ($B_1$, mesio-distal multiplanar view), ($B_2$, occluso-gingival view); CLSM images ($B_3$, the arrow indicates the Type D crack pattern).**

**Table 1 – The distribution percentages of ICDAS codes, demineralization levels, and microcrack patterns for all examined teeth.**

| | | | ICDAS | | | Total | Crack | | | | | Total |
|---|---|---|---|---|---|---|---|---|---|---|---|---|
| | | | 0 | 1 | 2 | | O | A | B | C | D | |
| DEM | 0 | Count | 91 | 0 | 0 | 91 | 59 | 31 | 1 | 0 | 0 | 91 |
| | | Column (%) | 100.0% | 0.0% | 0.0% | 100.0% | 64.8% | 34.1% | 1.1% | 0.0% | 0.0% | 100.0% |
| | | Row (%) | 98.9% | 0.0% | 0.0% | 46.4% | 54.1% | 53.4% | 9.1% | 0.0% | 0.0% | 46.4% |
| | I | Count | 1 | 33 | 9 | 43 | 22 | 17 | 4 | 0 | 0 | 43 |
| | | Column (%) | 2.3% | 76.7% | 20.9% | 100.0% | 51.2% | 39.5% | 9.3% | 0.0% | 0.0% | 100.0% |
| | | Row (%) | 1.1% | 78.6% | 14.5% | 21.9% | 20.2% | 29.3% | 36.4% | 0.0% | 0.0% | 21.9% |
| | II | Count | 0 | 9 | 24 | 33 | 12 | 7 | 6 | 4 | 4 | 33 |
| | | Column (%) | 0.0% | 27.3% | 72.7% | 100.0% | 36.4% | 21.2% | 18.2% | 12.1% | 12.1% | 100.0% |
| | | Row (%) | 0.0% | 21.4% | 38.7% | 16.8% | 11.0% | 12.1% | 54.5% | 100.0% | 28.6% | 16.8% |
| | III | Count | 0 | 0 | 29 | 29 | 16 | 3 | 0 | 0 | 10 | 29 |
| | | Column (%) | 0.0% | 0.0% | 100.0% | 100.0% | 55.2% | 10.3% | 0.0% | 0.0% | 34.5% | 100.0% |
| | | Row (%) | 0.0% | 0.0% | 46.8% | 14.8% | 14.7% | 5.2% | 0.0% | 0.0% | 71.4% | 14.8% |
| | Total | Count | 92 | 42 | 62 | 196 | 109 | 58 | 11 | 4 | 14 | 196 |
| | Column (%) | | 46.9% | 21.4% | 31.6% | 100.0% | 55.6% | 29.6% | 5.6% | 2.0% | 7.1% | 100.0% |
| | Row (%) | | 100.0% | 100.0% | 100.0% | 100.0% | 100.0% | 100.0% | 100.0% | 100.0% | 100.0% | |

## 4. Discussion

In this study, we observed the interproximal contact areas of freshly extracted maxillary and mandibular premolars using 3D SS-OCT, to investigate the association of enamel microcracks, observed by SS-OCT and CSLM, with demineralization, assessed using the ICDAS score and SS-OCT observation. We showed that ICDAS scores correlated significantly with demineralization level and microcrack patterns, and that significantly more demineralization and microcracks were present in the mesial side of maxillary than of mandibular premolars.

**Table 2 – The distribution of each parameter (ICDAS, DEM, and Crack) between the mesial and distal sides of maxillary and mandibular premolars.**

| | | U-M | | U-D | | L-M | | L-D | | p-value |
|---|---|---|---|---|---|---|---|---|---|---|
| | | n | % | n | % | n | % | n | % | |
| ICDAS | 0 | 13 | 26.5% | 24 | 49.0% | 29 | 59.2% | 26 | 53.1% | ≤0.001* |
| | 1 | 7 | 14.3% | 9 | 18.4% | 13 | 26.5% | 13 | 26.5% | |
| | 2 | 29 | 59.2% | 16 | 32.7% | 7 | 14.3% | 10 | 20.4% | |
| | Rank | A | | B | | B | | B | | |
| DEM | 0 | 13 | 26.5% | 23 | 46.9% | 29 | 59.2% | 26 | 53.1% | ≤0.001* |
| | I | 9 | 18.4% | 7 | 14.3% | 14 | 28.6% | 13 | 26.5% | |
| | II | 12 | 24.5% | 11 | 22.4% | 4 | 8.2% | 6 | 12.2% | |
| | III | 15 | 30.6% | 8 | 16.3% | 2 | 4.1% | 4 | 8.2% | |
| | Rank | A | | AB | | B | | B | | |
| Crack | O | 22 | 44.9% | 27 | 55.1% | 35 | 71.4% | 25 | 51.0% | 0.032* |
| | A | 16 | 32.7% | 14 | 28.6% | 11 | 22.4% | 17 | 34.7% | |
| | B | 4 | 8.2% | 2 | 4.1% | 2 | 4.1% | 3 | 6.1% | |
| | C | 1 | 2.0% | 2 | 4.1% | 0 | 0.0% | 1 | 2.0% | |
| | D | 6 | 12.2% | 4 | 8.2% | 1 | 2.0% | 3 | 6.1% | |
| | Rank | A | | AB | | B | | AB | | |

* significant at $p < 0.05$.

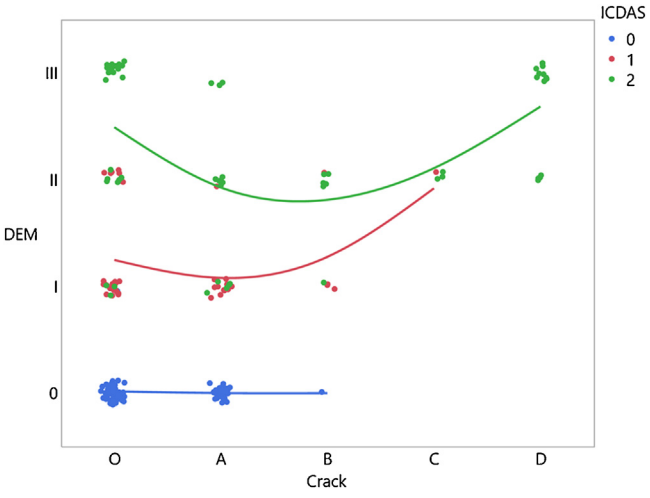


**Fig. 4 – Distribution of ICDAS codes, demineralization levels, and crack patterns. Lines indicate the distribution of the ICDAS code within the demineralization (DEM) and crack scores. blue: ICDAS code 0, red: ICDAS code 1, green: ICDAS code 2.**

Although the prevalence of caries experience increases with age, the highest caries rates at approximal surfaces in all age groups has been reported in a previous study [26]. Consequently, in order to attenuate the impact of an increase in age on our data, we used the teeth extracted for orthodontic purposes from young adults (18–35 years old) in this study.

The laser light source of SS-OCT, with a central wavelength of 1310 nm, can penetrate the entire thickness of enamel up to 3 mm [27]. Sound tooth surfaces at the interproximal contact area exhibit OCT signal reflectivity of the same level as that of the surrounding normal enamel, while demineralized areas can be detected as bright lesions due to the intensified backscatter signals [28,29]. Loss of minerals increases the enamel porosity. The micro-interfaces between mineral crystals created during demineralization and water within the pores cause higher reflectivity and results in increased brightness on OCT images [29,30]. During early enamel demineralization, low backscatter signals of the underlying sound enamel, due to the higher reflectivity from the superficial enamel, creates a visible lesion boundary [25]. Although the extent of demineralization was not quantitatively measured in this study, lesion demineralization was evaluated by dividing the enamel surface into three portions, from the outer surface to the DEJ. As the lesion pattern in proximal demineralization is cone-shaped (i.e., 3D in nature), the extent of the lesion was estimated by determining the deepest lesion boundary on the grayscale OCT images. The level of demineralization monitored determined in this way on 3D SS-OCT correlated significantly with ICDAS scores.

Besides the demineralized lesions, initial changes of enamel with internal microcracks localized at the contact zone were found (Fig. 2$A_1$, $B_1$ and Fig. 3$A_1$, $B_1$). Enamel microcracks appear as bright spots or bright lines due to the difference in refractive indices between enamel and the crack space, which increases the OCT signal [31]. Not all demineralized lesions in the interproximal contact areas were accompanied by microcracks: only 46% of examined teeth exhibited superficial enamel microcracks. The prevalence of such cracks may vary, depending on the characteristics of the individual's dentition, such as crowding, or spaces, and periodontal status. The patterns of microcracks found in the interproximal contact areas also differed from developmental enamel defects, such as lamella and enamel tufts.

In this study, the tooth surfaces were first comprehensively observed to detect cracks or damage caused during extraction. The microcracks in the enamel presented in this study were mostly localized within the subsurface enamel, and were not conventional macrocracks that extend from the outer enamel surface. The microcracks were frequently observed in the vicinity of the interproximal contact area, where no evidence of cracks were found with the naked eye. Conventional macrocracks are clinically found at the buccal or lingual tooth

crown portion, where self-care cleaning is easily accessible and caries are typically absent. The difference in anatomical location and oral health-care behavior should be taken into account. The enamel microcracks found in this study occurred in the posterior interdental areas, where access for cleaning devices is less optimal.

Segarra et al. [9] recently examined mastication-induced enamel crack behavior on the occlusal surfaces of cusps, by using 3D SS-OCT. When the enamel surface is subjected to compressive and impact forces, such as tensile or shear stress, during protrusive and lateral movement during mastication [13,32], superficial enamel cracks develop. Although masticatory forces do not directly affect the proximal contact area, these forces can be transmitted to the adjacent teeth along the arch [8–10]. Alexander et al. reported that physiological proximal contact is maintained by compressive force between the proximal surfaces of adjacent teeth and by resistance force when adjacent teeth passively touch each other, without force, to resist any separating force between them [33]. Furthermore, Benazzi et al. reported that occlusal compressive stresses result in tensile stress on the interproximal area of premolar teeth during masticatory loading, which was more aggressive in cases of advanced occlusal wear [34]. Interproximal attrition is influenced indirectly by the mastication forces applied on the teeth, in combination with the mesial force, producing tight interproximal contacts [8–11,35]. Therefore, the microcracks observed in the interproximal contact area are presumably induced by stress arising from the force of proximal tightness, which causes proximal attrition or increases the risk for enamel demineralization.

Internal microdefects (Type A) were predominantly detected on visually sound proximal contact areas, without any incidence of demineralization (Fig. 4). During mastication, the occlusal cusp of the antagonist jaw contacts the proximal ridge. This may cause small internal defects, which are observed as bright spots in the superficial subsurface enamel (Fig. 2$A_1$). This was clearly observed in confirmatory CLSM images (Fig. 2$A_3$).

Type B cracks were predominantly found in Types 1 and 2 demineralized lesions (Fig. 2$B_1$ and Fig. 4). During the initial stage of demineralization, the mechanical strength of enamel may decrease due to the dissolution of minerals and weakening of the inter-crystalline bonds [36]. Under such conditions, the proximal contact force during mastication could be a factor promoting the formation of a superficial crack along the long axis of the prism (Fig. 2$B_1$, $B_2$, $B_3$). This crack pattern can be likened to macro-fractures [36], in which lamella, a developmental enamel defect, can cause the crack to progress from the outer enamel towards the enamel tufts near the DEJ. The lamella may be a factor in the formation of such a crack pattern at the proximal surface, which may lead to the initiation of caries [14].

Type C cracks were only observed when demineralized lesions extended to the middle third of the enamel (Figs. 3 $A_1$, $A_2$, and 4). Demineralization causes a decrease in the toughness of enamel due to a deteriorated multi-level hierarchical structure [37,38]. These superficial transverse microcracks may have resulted from destruction and fragmentation of the enamel prisms within the lesion body, which in turn are exaggerated by proximal loading or by the deflection of a crack extending inward from the enamel surface, due to decussation of the prism [39]. Additionally, internal microdefects (Type A) may have interconnected due to enamel weakening by demineralization. This internal crack propagation can only be seen in the occluso-gingival view (Fig. 3$A_2$) and is difficult to confirm by CLSM imaging in a longitudinal section, due to the 3D nature of the crack (Fig. 3$A_3$).

Type D cracks were predominantly found when the demineralization had progressed to the inner third of the enamel layer (Fig. 3$B_1$, $B_2$, $B_3$). The crack runs from the outer enamel along the prism and then extends into the demineralized enamel lesion, which favors crack progression, as less energy is needed for the crack to progress through the inter-prismatic boundaries [39]. Although the outer surface layer of the enamel, with denser crystal apatite, appeared intact, microcrack formation in the underlying lesion body may lead to a breakdown of the enamel surface and formation of a cavitated lesion. This microcrack pattern observed with SS-OCT was confirmed with CLSM (Fig. 3$B_3$).

The mesial side of maxillary premolars presented a significantly higher frequency of demineralized lesions and their demineralization and crack analyses corresponded better with the ICDAS scores than did the mandibular premolars (Table 2). Proximal contact tightness in the maxilla is greater than that in the mandible during clenching [11]; thus, occlusal forces may have a greater effect on maxillary teeth than on mandibular teeth. This assumption agrees with the finding of another study, in which the prevalence of non-carious cervical lesions was higher in maxillary premolars, due to higher occlusal forces [40]. In addition to higher occlusal stress, lower intraoral salivary flow [41] and broader contact areas [42] might explain the higher frequency of demineralized lesions and crack formation in maxillary premolars.

Our study had some limitations. First, the use of extracted teeth, which may have been subjected to certain forces during the extraction procedure, could have affected the outcome. Second, although SS-OCT was clinically used to detect interproximal caries through the overlying occlusal and marginal ridge structure as it produces sufficient backscatter signals [25], future in-vivo studies are needed to confirm the preliminary results of our study.

## 5. Conclusion

The incidence of enamel microcracks at the proximal contact area of teeth increased in relation to demineralization, and may act as a predisposing factor for proximal caries progression. Additionally, this study demonstrated that 3D SS-OCT is a valuable diagnostic tool for comprehensive assessment of microstructural changes in enamel, such as demineralization and cracks development.

## Acknowledgments

This research project was supported by the Research Grant for Longevity Science (29-3) Ministry of Health, Labor and Welfare, Japan and by Grant-in-Aid for Scientific Research (16K11544) from the Japan Society for the Promotion of Science (JSPS).

## REFERENCES


[1] Pitts NB, Zero DT, Marsh PD, Ekstrand K, Weintraub JA, Ramos-Gomez F, et al. Dental caries. Nat Rev Dis Prim 2017;3, http://dx.doi.org/10.1038/nrdp.2017.30.

[2] Beltrán-Aguilar ED, Barker LK, Canto MT, Dye BA, Gooch BF, Griffin SO, et al. Surveillance for dental caries, dental sealants, tooth retention, edentulism, and enamel fluorosis — United States, 1988–1994 and 1999–2002. J Can Dent Assoc (Tor) 2005;54(3):1–43.

[3] Tranaeus S, Shi XQ, Angmar-Mansson B. Caries risk assessment: methods available to clinicians for caries detection. Community Dent Oral Epidemiol 2005;33:265–73, http://dx.doi.org/10.1111/j.1600-0528.2005.00234.x.

[4] Bourgeois D, David A, Inquimbert C, Tramini P, Molinari N, Carrouel F. Quantification of carious pathogens in the interdental microbiota of young caries-free adults. PLoS One 2017;12(10):e0185804, http://dx.doi.org/10.1371/journal.pone.0185804.

[5] Hugoson A, Koch G, Slotte C, Bergendal T, Thorstensson B, Thorstensson H. Caries prevalence and distribution in 20–80-year-olds in Jönköping, Sweden, in 1973, 1983, and 1993. Community Dent Oral Epidemiol 2000;28:90–6, http://dx.doi.org/10.1034/j.1600-0528.2000.028002090.x.

[6] Hopcraft MS, Morgan MV. Comparison of radiographic and clinical diagnosis of approximal and occlusal dental caries in a young adult population. Community Dent Oral Epidemiol 2005;33:212–8, http://dx.doi.org/10.1111/j.1600-0528.2005.00216.x.

[7] Allison PJ, Schwartz S. Interproximal contact points and proximal caries in posterior primary teeth. Pediatr Dent 2003;25:334–40.

[8] Dörfer CE, Von Bethlenfalvy ER, Staehle HJ, Pioch T. Factors influencing proximal dental contact strengths. Eur J Oral Sci 2000;108:368–77, http://dx.doi.org/10.1034/j.1600-0722.2000.108005368.x.

[9] Southard TE, Southard KA, Tolley EA. Variation of approximal tooth contact tightness with postural change. J Dent Res 1990;69(11):1776–9, http://dx.doi.org/10.1177/00220345900690111301.

[10] Oh SH, Nakano M, Bando E, Keisuke N, Shigemoto S, Jeong JH, et al. Relationship between occlusal tooth contact patterns and tightness of proximal tooth contact. J Oral Rehabil 2006;33:749–53, http://dx.doi.org/10.1111/j.1365-2842.2006.01635.x.

[11] Oh SH, Nakano M, Bando E, Shigemoto S, Kori M. Evaluation of proximal tooth contact tightness at rest and during clenching. J Oral Rehabil 2004;31:538–45, http://dx.doi.org/10.1111/j.1365-2842.2004.01181.x.

[12] Simon J. Biomechanically-induced dental disease. Gen Dent 2000;48(5):598–605.

[13] Segarra MS, Shimada Y, Sadr A, Sumi Y, Tagami J. Three-dimensional analysis of enamel crack behavior using optical coherence tomography. J Dent Res 2016;96(3):308–14, http://dx.doi.org/10.1177/0022034516680156.

[14] Walker BN, Makinson OF, Peters MGRB. Enamel cracks. The role of enamel lamellae in caries initiation. Aust Dent J 1998;43:110–6, http://dx.doi.org/10.1111/j.1834-7819.1998.tb06099.x.

[15] Gimenez T, Piovesan C, Braga MM, Raggio DP, Deery C, Ricketts DN, et al. Visual inspection for caries detection: a systematic review and meta-analysis. J Dent Res 2015;94:895–904, http://dx.doi.org/10.1177/0022034515586763.

[16] Schwendicke F, Tzschoppe M, Paris S. Radiographic caries detection: a systematic review and meta-analysis. J Dent 2015;43:924–33, http://dx.doi.org/10.1016/j.jdent.2015.02.009.

[17] Wenzel A, 83 Spec No C:C72-75 Bitewing and digital bitewing radiography for detection of caries lesions. J Dent Res 2004, http://dx.doi.org/10.1177/154405910408301S14.

[18] Ismail A, Sohn W, Tellez M. The International Caries Detection and Assessment System (ICDAS): an intergrated system for measuring dental caries. Community Dent Oral Epidemiol 2007;3:170–8, http://dx.doi.org/10.1111/j.1600-0528.2007.00347x.

[19] Ekstrand KR, Luna LE, Promisiero L, Cortes A, Cuevas S, Reyes JF, et al. The reliability and accuracy of two methods for proximal caries detection and depth on directly visible proximal surfaces: an in vitro study. Caries Res 2011;45(2):93–9, http://dx.doi.org/10.1159/000324439.

[20] Machoy M, Seeliger J, Szyszka-Sommerfeld L, Koprowski R, Gedrange T, Woźniak K. The use of optical coherence tomography in dental diagnostics: a state-of-the-art review. J Healthc Eng 2017;2017:7560645, http://dx.doi.org/10.1155/2017/7560645.

[21] Hsieh Y-S, Ho Y-C, Lee S-Y, Chuang C-C, Tsai J, Lin K-F, et al. Dental optical coherence tomography. Sensors 2013;13:8928–49, http://dx.doi.org/10.3390/s130708928.

[22] Shimada Y, Sadr A, Burrow MF, Tagami J, Ozawa N, Sumi Y. Validation of swept-source optical coherence tomography (SS-OCT) for the diagnosis of occlusal caries. J Dent 2010;38:655–65, http://dx.doi.org/10.1016/j.jdent.2010.05.004.

[23] Hayashi J, Shimada Y, Tagami J, Sumi Y, Sadr A. Real-time imaging of gap progress during and after composite polymerization. J Dent Res 2017;96:992–8, http://dx.doi.org/10.1177/0022034517709005.

[24] Nakagawa H, Sadr A, Shimada Y, Tagami J, Sumi Y. Validation of swept source optical coherence tomography (SS-OCT) for the diagnosis of smooth surface caries in vitro. J Dent 2013;41:80–9, http://dx.doi.org/10.1016/j.jdent.2012.10.007.

[25] Shimada Y, Nakagawa H, Sadr A, Wada I, Nakajima M, Nikaido T, et al. Noninvasive cross-sectional imaging of proximal caries using swept-source optical coherence tomography (SS-OCT) in vivo. J Biophotonics 2014;7:506–13, http://dx.doi.org/10.1002/jbio.201200210.

[26] Demirci M, Tuncer S, Yuceokur AA. Prevalence of caries on individual tooth surfaces and its distribution by age and gender in university clinic patients. Eur J Dent 2010;4(3):270–9, http://dx.doi.org/10.1016/j.pmcj.2009.04.001.

[27] Jones RS, Darling CL, Featherstone JDB, Fried D. Imaging artificial caries on the occlusal surfaces with polarization-sensitive optical coherence tomography. Caries Res 2006;40(2):81–9, http://dx.doi.org/10.1159/000091052.

[28] Fried D, Glena RE, Featherstone JD, Seka W. Nature of light scattering in dental enamel and dentin at visible and near-infrared wavelengths. Appl Opt 1995;34(7):1278–85, http://dx.doi.org/10.1364/AO.34.001278.

[29] Darling CL, Huynh GD, Fried D. Light scattering properties of natural and artificially demineralized dental enamel at 1310 nm. J Biomed Opt 2006;311(3):34023, http://dx.doi.org/10.1117/1.2204603.

[30] Hariri I, Sadr A, Shimada Y, Tagami J, Sumi Y. Effects of structural orientation of enamel and dentine on light attenuation and local refractive index: an optical coherence tomography study. J Dent 2012;40(5):387–96, http://dx.doi.org/10.1016/j.jdent.2012.01.017.

[31] Imai K, Shimada Y, Sadr A, Sumi Y, Tagami J. Noninvasive cross-sectional visualization of enamel cracks by optical coherence tomography in vitro. J Endod 2012;38(9):1269–74, http://dx.doi.org/10.1016/j.joen.2012.05.008.

[32] Lucas PW, Van Casteren A. The wear and tear of teeth. Med Princ Pract 2015;24:3–13, http://dx.doi.org/10.1159/000367976.

[33] Vardimon AD, Matsaev E, Lieberman M, Brosh T. Tightness of dental contact points in spaced and non-spaced permanent

dentitions. Eur J Orthod 2001;23(3):305–14, http://dx.doi.org/10.1093/ejo/23.3.305.
[34] Benazzi S, Nguyen HN, Schulz D, Grosse IR, Gruppioni G, Hublin JJ, et al. The evolutionary paradox of tooth wear: simply destruction or inevitable adaptation? PLoS One 2013;8:1–12, http://dx.doi.org/10.1371/journal.pone.0062263.
[35] Sarig R, Hershkovitz I, Shpack N, May H, Vardimon AD. Rate and pattern of interproximal dental attrition. Eur J Oral Sci 2015;123:276–81, http://dx.doi.org/10.1111/eos.12198.
[36] Kunin AA, Evdokimova AY, Moiseeva NS. Age-related differences of tooth enamel morphochemistry in health and dental caries. EPMA J 2015;6:1–11, http://dx.doi.org/10.1186/s13167-014-0025-8.
[37] He LH, Swain MV. Understanding the mechanical behaviour of human enamel from its structural and compositional characteristics. J Mech Behav Biomed Mater 2008;1:18–29, http://dx.doi.org/10.1016/j.jmbbm.2007.05.001.
[38] Leal NMS, Silva JL, Benigno MIM, Bemerguy EA, Meira JBC, Ballester RY. How mechanical stresses modulate enamel demineralization in non-carious cervical lesions? J Mech Behav Biomed Mater 2017;66:50–7, http://dx.doi.org/10.1016/j.jmbbm.2016.11.003.
[39] Bajaj D, Nazari A, Eidelman N, Arola DD. A comparison of fatigue crack growth in human enamel and hydroxyapatite. Biomaterials 2009;29(36):4847–54, http://dx.doi.org/10.1016/j.biomaterials.2008.08.019.A.
[40] Igarashi Y, Yoshida S, Kanazawa E. The prevalence and morphological types of non-carious cervical lesions (NCCL) in a contemporary sample of people. Odontology 2017;105(4):443–52, http://dx.doi.org/10.1007/s10266-017-0300-y.
[41] Humphrey SP, Williamson RT. A review of saliva: normal composition, flow, and function. J Prosthet Dent 2001;85:162–9, http://dx.doi.org/10.1067/mpr.2001.113778.
[42] Gohil KS, Talim ST, Singh I. Proximal contacts in posterior teeth and factors influencing interproximal caries. J Prosthet Dent 1973;30(3):295–302, http://dx.doi.org/10.1016/0022-3913(73)90186-8.